OMICS A Journal of Integrative Biology
Volume 19, Number 2, 2015

DOI: 10.1089/omi.2014.0137

Next Generation Design, Development, and Evaluation of Cryoprobes for Minimally Invasive Surgery and Solid Cancer Therapeutics: In Silico and Computational Studies

Abdul Mateen A.G. Shaikh, Atul Srivastava, and M.D. Atrey

Abstract

Cryosurgery is a widely regarded minimally invasive surgery for treatment of various types of cancers. It involves destruction of cancer cells within a limited spatial domain by exposing them to very low temperatures while minimizing injury to surrounding peripheral healthy tissues. Surprisingly, despite increasing demands for cryosurgery, there has been limited innovation in the design of cryoprobes, particularly in solid tumors (e.g., breast, prostate, and lung cancers). For advances in cancer therapeutics, integrative biology research can illuminate the mechanistic interface between a surgical cryoprobe and its tissue site of action. Here, we describe the design and development of three novel low pressure liquid nitrogen (LN2) cryoprobes with different physical dimensions and the parameters that determine their effectiveness experimentally, using water and biogel as the phase changing mediums. Smaller diameter low pressure probes produced lesser cryogenic injury. Vapor Separator is found to be an effective means (particularly for smaller diameter probes) to remove the vapor lock in the LN2 low pressure cryoprobes and also to reduce the precooling time. The low pressure LN2 cryoprobes produced lower probe temperatures and consequently larger and faster iceball growth for low cooling loads. Additionally, a numerical code was written in MATLAB based on the Enthalpy method to simulate the bio-heat transfer in a cryosurgical process. The numerical code is validated by analytical solution, laboratory experiments, and data from an *in vivo* cryosurgery. The developed numerical code is presented herein to illustrate that LN2 cryoprobes capable of producing lower probe temperatures produce more efficient cryosurgical operation by reducing the buffer zone and duration of surgery.This is the first report, to the best of our knowledge, on design of the next generation of LN2 surgical cryoprobes. These new surgical cryoprobes offer potentials for future preclinical and clinical testing in solid cancers.

Introduction

Cryosurgery is an emerging field and holds a great deal of promise as an alternative option in the domain of minimally invasive surgery. Cryosurgery involves destruction of cancerous or unwanted cells by exposing them to cryogenic temperatures that are produced either from a Joule Thomson expansion device or using a cryogen such as liquid nitrogen. The cryogenic temperatures are applied using a hollow tube device called cryoprobe. The main aim of any cryosurgical process is to destroy the cells within the tumor region while minimizing the damage to the surrounding healthy tissue. The growth of the iceball around the cryoprobe is monitored via an ultrasound or a MRI (Rubinsky, 2000). A standard cryosurgical protocol includes freezing, followed by thawing and then if necessary, repetition of the freeze thaw cycle.

Surprisingly, despite increasing demands for cryosurgery, there has been limited innovation in the design of cryoprobes, particularly in solid tumors (e.g., breast, prostate, and lung cancers). For advances in cancer therapeutics, integrative biology research can illuminate the mechanistic interface between a surgical cryoprobe and its tissue site of action. Importantly, understanding the determinants of the cell destruction involved in a cryosurgical procedure can lay down an efficient cryosurgical protocol.

This is an interdisciplinary bioengineering research article that contributes to the next generation design of surgical cryoprobes. In order to offer the necessary background to the reader on cryoprobes, in a way suitable for an interdisciplinary

Department of Mechanical Engineering, IIT Bombay, Powai, Mumbai, India.

readership in integrative biology and biomedicine, we present below a concise background on cryoprobes and the way they were designed thus far. This lays a solid foundation for the readers to better contextualize the new findings emerging from the present report for the next generation design of cryoprobes in cancer therapeutics.

Cryoprobes and their mechanism of action

In general, there are a number of different mechanisms that cause cryoinjury and the complex interplay of these mechanisms ultimately defines the outcome of a cryosurgical process. Cell destruction mechanisms can be broadly classified as follows:

1. Direct cellular injury
   a. Hypothermia
   b. Freezing injury
      i. Extracellular ice crystallization or the solution effect
      ii. Intracellular ice crystallization (IIF)
2. Delayed injury or vascular stasis
3. Apoptosis

Solution effect is the lethal effect of high concentration of solutes within the cell when exposed to low cooling rates. *IIF* is a more lethal mode of destruction occurring at high cooling rates, which results in ice formation within the cells, thus destroying it completely. *Vascular stasis* is the result of the damage to the vasculature, especially the endothelial layer of the blood vessels. *Stagnation* of blood flow to the frozen region occurs post thawing and deprives the cells of any chance of survival. Mechanisms such as *hypothermia* and *apoptosis* play an inconsistent or an insufficient role in cryoinjury.

Owing to the complex nature of cell destruction mechanisms, literature proposed by Gage and Baust (1988) suggests the use of a certain minimum temperature (called the critical temperature) as a benchmark to ensure complete destruction of cells, mainly through the mechanism of IIF. This critical temperature depends on the cell type being frozen. In general, a temperature of $-50^{\circ}C$ can be assumed to be a safe critical temperature for most types of cancerous cells. The volumetric extent of the critical isotherm must envelope the tumor. The volume of the 'buffer zone' that extends beyond the critical isotherm up to the phase change temperature of the frozen tissue is kept as small as possible to ensure minimum damage to the healthy tissue.

Monitoring of the iceball growth is necessary to avoid any under freezing or over freezing of the cancerous tissue. The commonly used imaging techniques by Rubinsky (2000) such as MRI and ultrasound fail to image or monitor the critical isotherm. Most imaging or monitoring techniques either image the freezing front or monitor the temperature at certain specific locations, unaware of the temperature gradients within the iceball. Thus, the precision of the process is affected. Numerical simulations prove to be very useful in overcoming this drawback by estimating the critical isotherm and can be used in optimizing the cryosurgical process and also aid in the design and development of cryoprobes.

Joule Thomson cryoprobes and liquid nitrogen (LN_2) cryoprobes are the most widely used cryoprobes in cryosurgery. Joule Thomson cryoprobes in general are not able to reach the very low temperatures required in cancer treatment; however with the current advances in mixed gas J-T cooling, this drawback could be overcome. LN_2 cryoprobes on the other hand can produce very low temperatures and have a higher cooling capacity. Such cryoprobes are therefore more relevant in cancer treatment; since they can induce the IIF mode of cell destruction in a larger volume of the frozen region. LN_2 cryoprobes however lack the non-invasiveness of the J-T cryoprobes and also suffer from insulation problems and require high precooling time.

The fluid flow and heat transfer inside a LN_2 cryoprobe is in general a complex transient phenomenon involving unstable flow and phase change heat transfer; thus making the freezing process hard to control and to give accurate prediction about the tumor temperature.

Initially, in an LN_2 cryoprobe, there is only gas flow owing to the large heat flux between the flow and the surroundings. But as the temperature drops, the heat transferred to the transport pipe can no longer evaporate all the LN_2 inside and LN_2 droplets can exist in the inlet N_2 gas flow. This flow pattern is called droplet flow or mist flow. When the liquid phase takes up more and more space, it forms a thin film adhering to the pipe wall, and the gas begins to aggregate in the center of the tube to become two-phase annular flow. These flow patterns vary with time of surgery, size of the cryoprobe, cooling loads, etc. Thus the complex heat transfer and fluid flow inside a LN_2 cryoprobe makes it difficult to model it mathematically, and recourse to experimental methods is advantageous. Most commercial LN_2 cryoprobes are high pressure probes with pressures of the order of 15 bar or more. The disadvantage of such cryoprobes is that they are not safe. The high pressure also increases the boiling point of LN_2. Low pressure LN_2 croyoprobes are safe and lack the complexity of high pressure LN_2 probes or even the sub-cooled LN_2 probes.

Aims of the present research

The work presented here is concerned with developing low pressure LN_2 cryoprobes using experimental work. A numerical code is also developed based on the enthalpy method to aid in the development of LN_2 cryoprobes. The numerical code is validated with laboratory experiments and also with the data available in literature. The computational *in silico* and empirical approach used here is directly relevant to the readers in the area of integral biology.

Materials and Methods

Development of low pressure LN_2 cryoprobe

During the experimental work, three low pressure LN_2 cryoprobes were built in regards to Probe1, Probe2, and Probe3. The inlet pressure in all the three probes is kept at 2.2 bar absolute and the outlet pressure is atmospheric. The basic construction of the probes consists of two concentric hollow tubes. LN_2 enters the inner tube at one end and is released at the other end in the annular space between the two tubes where it gains heat from the surrounding tissue and changes phase. The resulting two phase mixture then passes through the annular space and is released into the atmosphere. Another concentric tube or the vacuum tube envelopes the outer tube except at a certain length on the tip of the cryoprobe (cryogenic section of the cryoprobe). The annular space covered between the outer tube and the vacuum tube is vacuum insulated to prevent damage to the surrounding healthy tissue. The cryogenic section of the probe comes in contact with the tumor and exchanges heat with it.

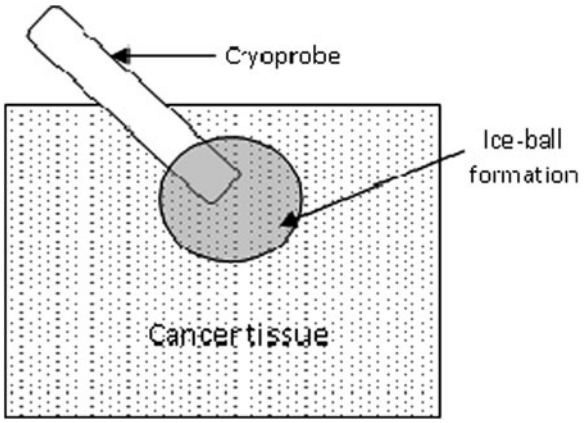

FIG. 1. Concept of cryosurgery for ultra-low temperature medical devices. The parameters of the probe-iceball formations are of interest as the iceball is the precursor crucial for cell destruction and thus for cancer therapeutics.

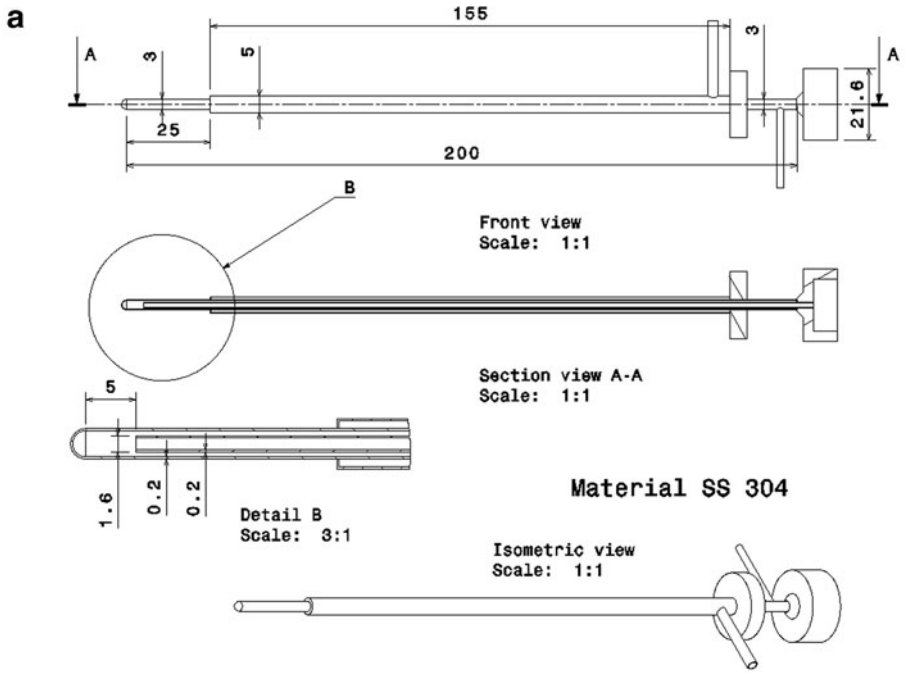

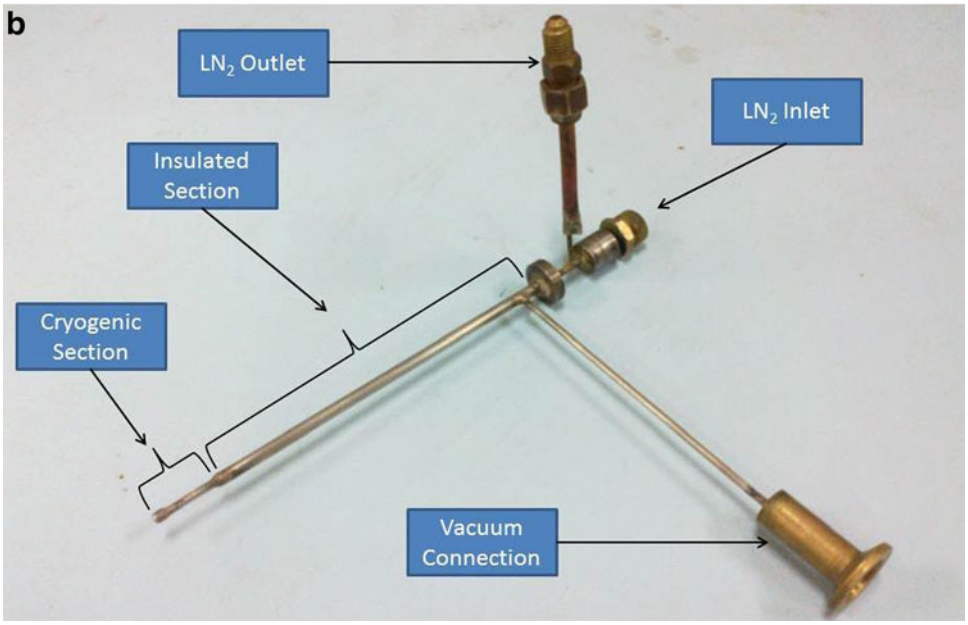

FIG. 2. Design of next generation cryosurgery probe (Probe2).

Figure 1 shows the schematic representation of the concept of cryosurgery for ultra-low temperature medical devices. The construction details of Probe1, developed in the present work, are shown in Figure 2. The diameter of the cryogenic section of the probe is 3 mm and that of the vacuum insulated section is 5 mm. All the cryoprobes are made of stainless steel SS304 to make them safe and reliable for both the patient and the surgeon.

Construction details of Probe2 are shown in Figure 3. The diameter of the cryogenic section of the probe is 3 mm and that of the vacuum insulated section is increased to 12.7 mm.

Construction details of Probe3 are shown in Figure 4. The diameter of the cryogenic section of the probe is increased to 11 mm and the vacuum insulated section is tapered out to increase the non-invasiveness.

Low pressure LN_2 cryoprobes of smaller diameters face the problem of vapor lock in the cryogenic section. Due to high cooling loads, there is instantaneous evaporation of LN_2 in the cryogenic section of the probe. This results in a high back pressure on the system. This back pressure may be so high that it may not allow any flow of liquid. To overcome this problem, a vapor separator is attached to the inlet of the cryoprobe. The details of the vapor separator are shown in Figure 5.

The vapor separator consists of a hollow chamber connected to the inlet of the cryoprobe. At the top of the vapor separator, a vent valve is placed. The vapor separator has two fold functions; first it provides a path to release the excessive pressure created by the vapor lock, and second it acts as a vent for the gaseous N2 produced as a result of inefficient insulation in the inlet liquid line. There is however a drawback associated with such a configuration. There is no control over the amount of LN2 by passed through the vent valve of the vapor separator. The excessive back pressure may force most of the incoming LN2 to vent valve and only a small amount would then reach the cryogenic section of the probe.

Experimental set up

Experiments were conducted to evaluate the performance of the LN2 cryoprobes and also to validate the numerical model presented in the next section. Figure 6 shows the schematic diagram of the basic experimental set up.

The experimental set-up consists of four parts

- LN2 Supply
- Cryoprobe
- Iceball monitoring and instrumentation
- Phase changing medium

LN2 is transferred from the LN2 dewar to the cryoprobe at a pressure of 2.2 bar absolute. Probes 1 and 2 are attached with the vapor separator for removing the vapor lock and reducing the precooling time of the cryoprobes. Probe3 is run

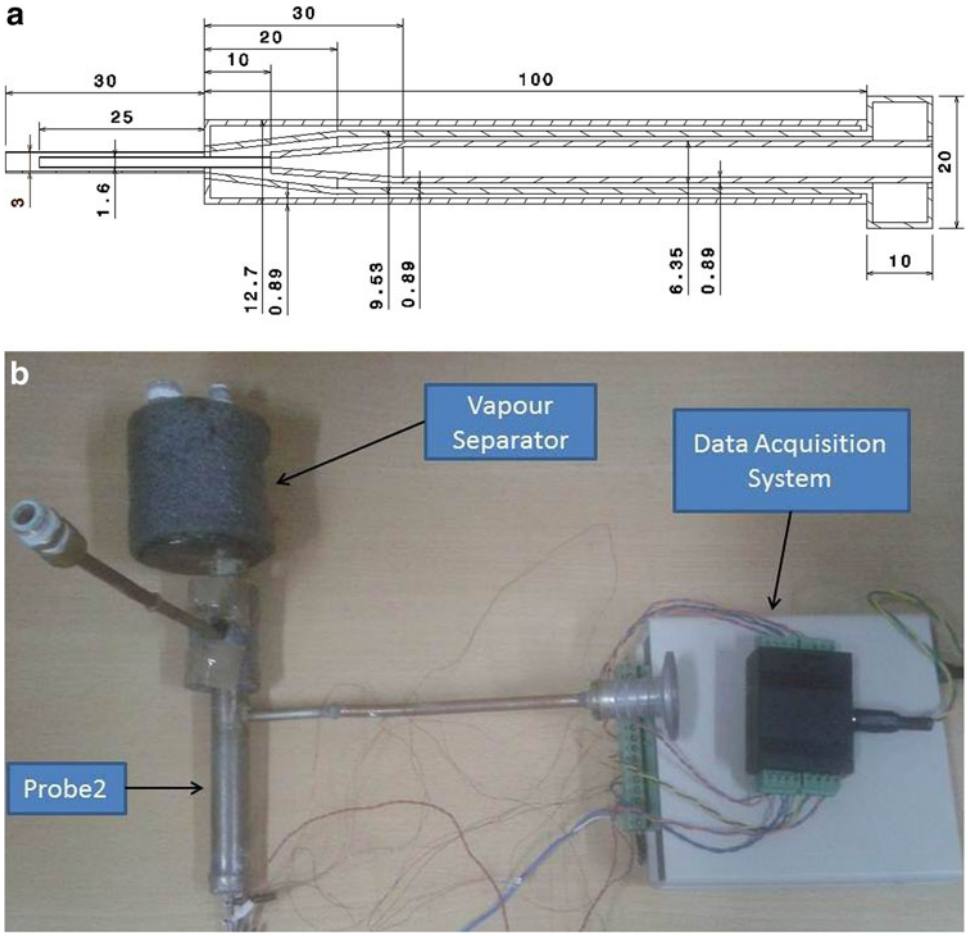

FIG. 3. Details of Probe2.

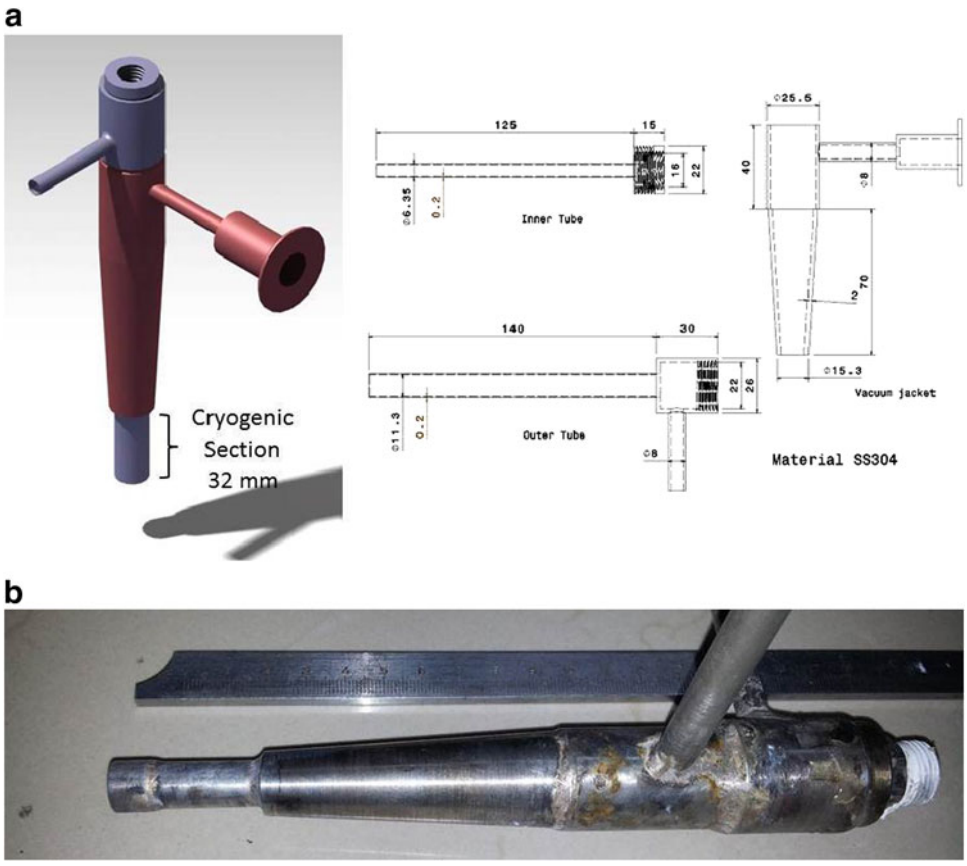

FIG. 4. Details of Probe3.

without any vapor separator since the large diameter of Probe3 is assumed to prevent formation of any vapor lock. Vacuum pump is used to thermally insulate the vacuum section of the LN2 probe. Typical vacuum attained in the vacuum jacket of the cryoprobe is of the order of 10^{-3} mbar. PT100 resistance temperature sensors are used to gauge the iceball growth and the probe surface temperature. Temperature sensors are placed on the cryogenic section of the probe and along certain radial distance of the probe for iceball monitoring, as shown in Figure 7.

The probe sensors and the last radial sensor (sensor T3 in Fig. 7) act as the boundary conditions in the numerical model

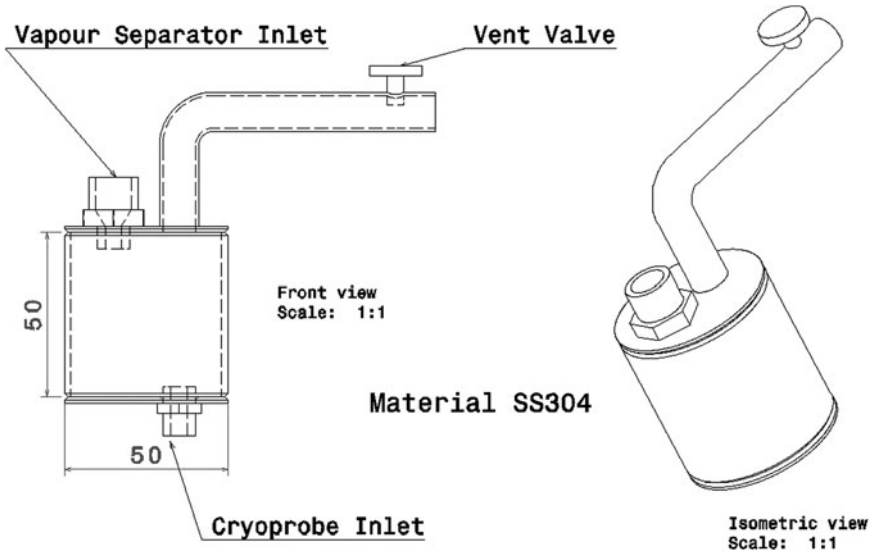

FIG. 5. Details of vapor separator.

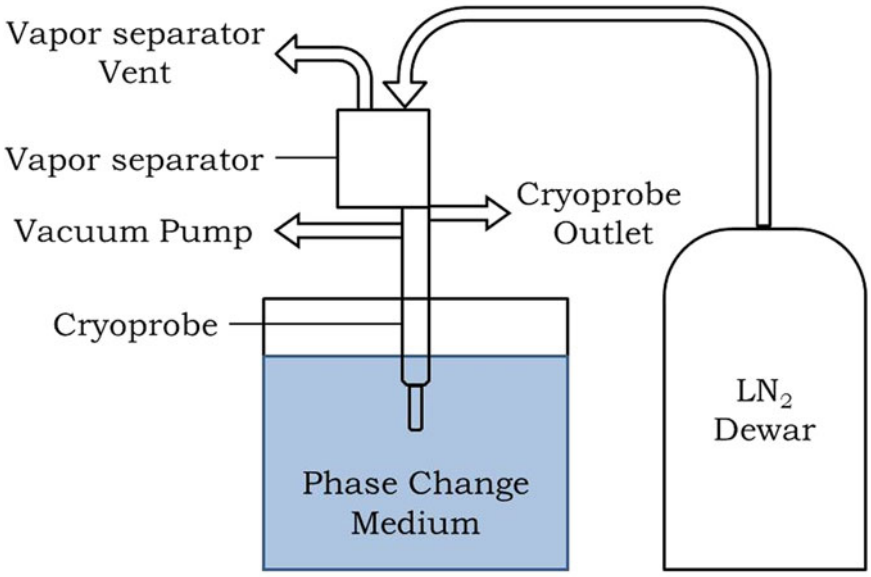

FIG. 6. Schematic of experimental set up.

and the remaining radial sensors are used for code validation. Since the diameters of the iceball produced are about 40 mm, large sized sensors can disturb the thermal profile of the iceball by conducting in heat. The sensing region of each PT100 sensor is a square section of about 1 mm^2 attached to two thin insulated leads. It is assumed that the thermal mass of the PT100 sensors is small enough to neglect any disturbances in the thermal profile of the iceball. The temperature sensors are positioned by tying them with a thin thread; this is again done to minimize the disturbance to the thermal field caused by the invasive iceball monitoring technique.

Considering the fact that the cells are composed of more than 90% of water, the *in vitro* experiments are conducted in two types of phase changing medium viz.

- Water
- Bio-gel: 0.1% agarose solution in water

The phase changing mediums do not simulate the actual biological tissue in terms of the metabolism and blood perfusion heat source. Water as a phase change medium will produce some convection effects that are not considered in the numerical model. The bio-gel is made by dissolving 1 g of SRL Agarose powder in 1 liter of distilled water. The agarose content in the bio-gel is kept at 0.1% to enhance the visibility of the growth of iceball without compromising much on the gel strength. At such low concentrations of agarose, the bio-gel is assumed to have properties similar to that of water. Convective currents do not occur in the bio-gel owing to its gel structure.

Numerical model

A numerical code is written in MATLAB for 1D and 2D numerical analysis of the bio heat transfer in cryosurgery. The most widely used Penne's bio-heat transfer equation from Pennes (1948) is used for numerical modeling.

Biological tissues are considered to be non-ideal materials that change phase over a range of temperature, whereas pure

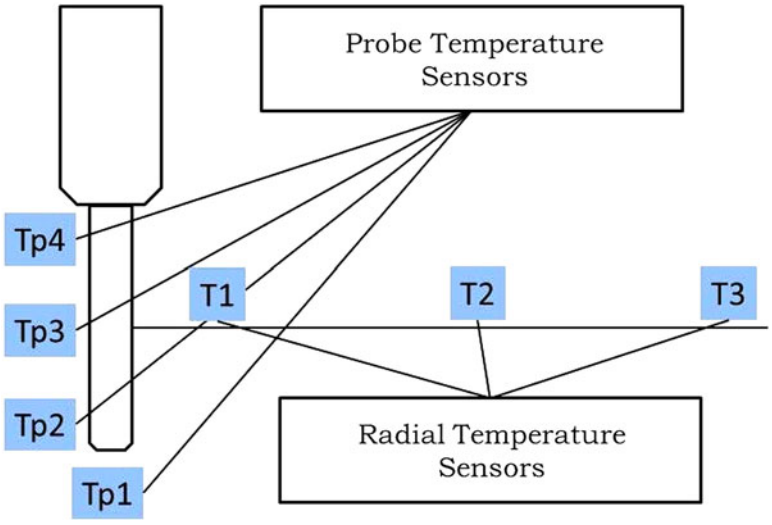

FIG. 7. Temperature sensor location.

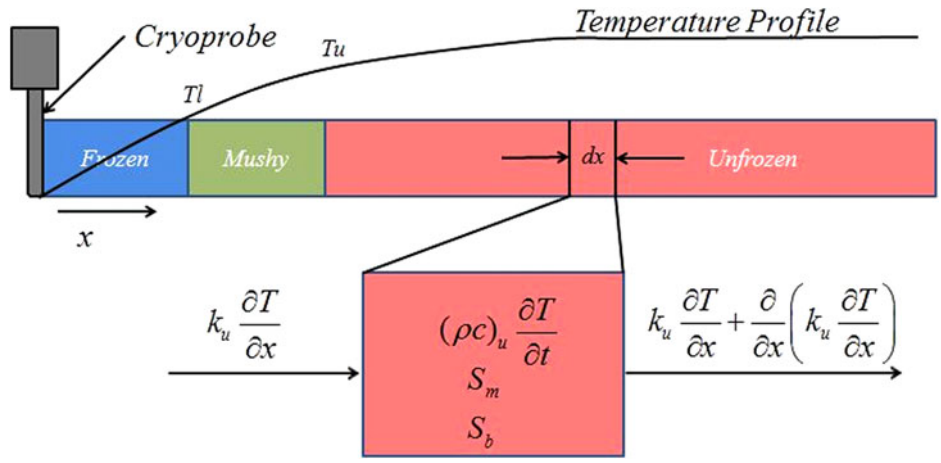

FIG. 8. 1D Cryo-freezing process.

materials such as water is considered to be an ideal material as it changes phase at a constant temperature. Considering the low concentrations of agarose in the bio-gel, it is assumed to have the same biophysical properties as that of water during the numerical analysis. Numerical simulations are done for three phase changing mediums viz. water, bio ge, and biological tissue. A one dimensional cryo-freezing process for a biological tissue is shown in Figure 8. The cryoprobe is placed at x = 0, and the other end of the tissue (at a sufficiently long distance from the probe) is assumed to be adiabatic. At any instant the lower and upper phase change interfaces are at T_l and T_u, respectively, and they define the three regions that are unfrozen region (subscript *u*), frozen region (subscript *f*), and the two phase or mushy region (subscript *i*).

The Penne's bio heat transfer equation is given as follows

$$\rho c \frac{\partial T}{\partial t} = \nabla k \nabla T + S_m + S_b \qquad \text{(Eq. 1)}$$

where T is the tissue temperature, ρ is the density of tissue, and c is its specific heat. S_m is the metabolism heat source per unit volume of the tissue and S_b is the blood perfusion heat source defined as follows

$$S_b = (\rho c)_b \ \omega_a (T_b - T) \qquad \text{(Eq. 2)}$$

where 'ω_a' is the blood perfusion rate per unit volume of tissue and T_b is the arterial temperature. The heat sources are absent in the mushy and frozen region

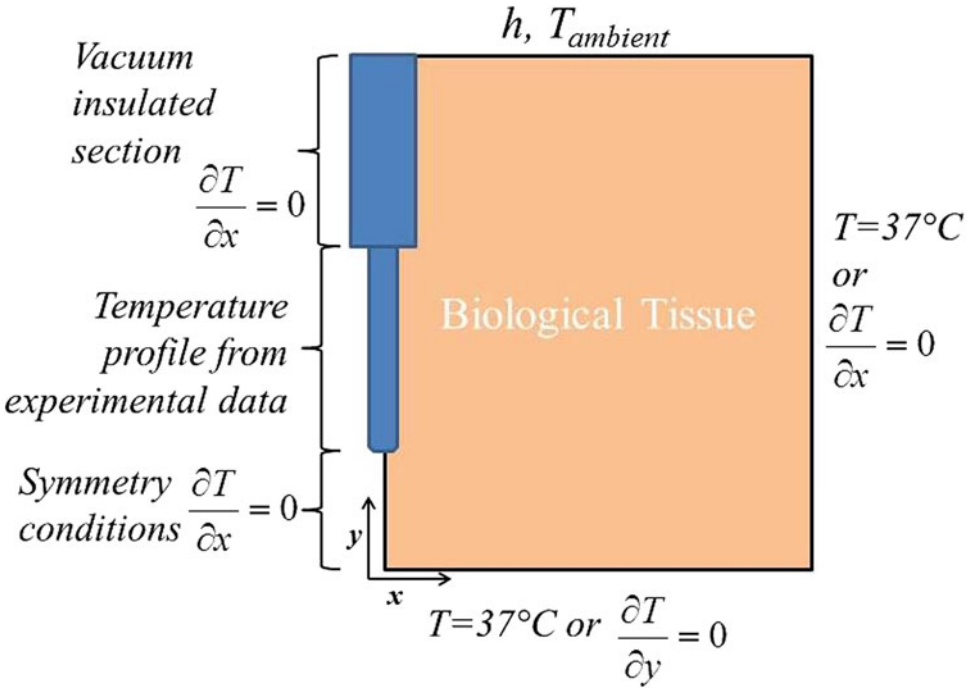

FIG. 9. Typical boundary conditions used in 2D numerical simulations.

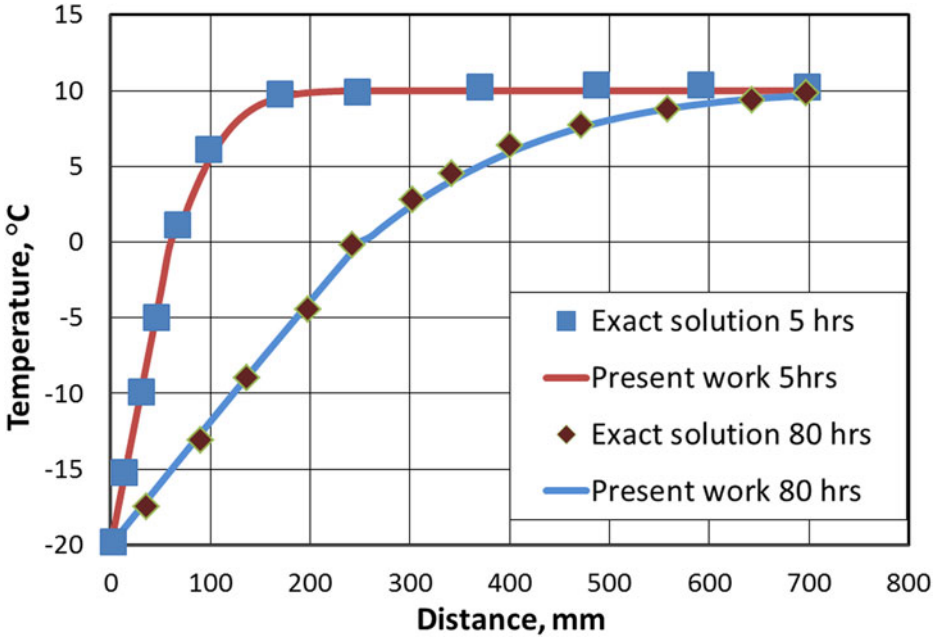

FIG. 10. Comparison of numerical code with analytical solution (Lee and Bastacky, 1995) for water freezing.

Enthalpy method

Equation 1 comes under the class of moving boundary problems for phase change heat transfer. In general, their analytical solution is difficult to obtain for real life problems, and numerical methods are preferred. The enthalpy method is the easiest and the most widely used fixed grid technique for phase change heat transfer problems. The current numerical code used for simulating cryosurgery is written based on the enthalpy method. The basic idea is to define an enthalpy function as shown in the following equation and then substitute it in the bio heat equation.

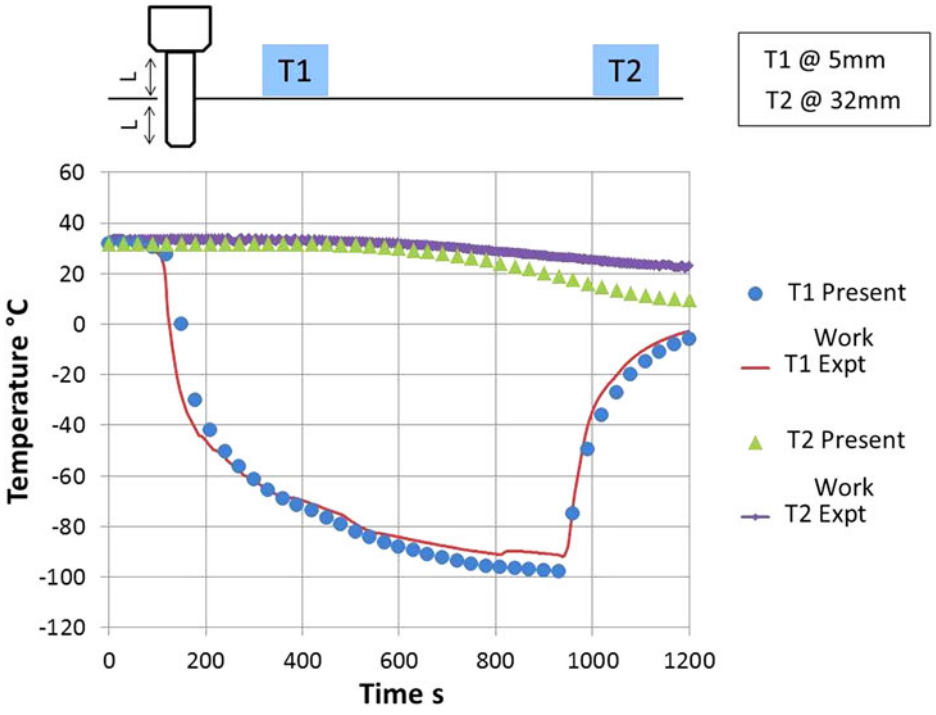

FIG. 11. Comparison of numerical model with bio-gel cryo-freezing experiment using Probe2 and vapor separator.

TABLE 1. THERMO-PHYSICAL PROPERTIES USED FOR PORCINE LIVER CRYOSURGERY SIMULATION

Upper phase change Temperature T_u	-1°C
Lower phase change Temperature T_l	-10°C
Unfrozen tissue density	1000 kg/m^3
Frozen tissue density	998 kg/m^3
Unfrozen tissue thermal conductivity k_u	0.50208 W/m-K
Frozen tissue thermal conductivity k_f	1.75728 W/m-K
Unfrozen tissue Specific heat c_u	3347.2 J/kg-K
Frozen tissue Specific heat c_f	1673.6 J/kg-K
Blood Specific heat C_b	3.822 MJ/m^3-K
Artery blood temperature T_b	37°C
Body core temperature	37°C
Latent heat LH (for soft tissue)	250 MJ/m^3
Blood perfusion of tissue ω_a	0.01872 ml/s-ml
Metabolic rate S_m (for soft tissue)	4.2 kW/m^3

$$H(T)=\begin{cases}\int_{T_{ref}}^{T} C_f dT & T\le T_l\\ \int_{T_{ref}}^{T_l} C_f dT+\int_{T_l}^{T}(C_i+L)dT & T_l\le T\le T_u\\ \int_{T_{ref}}^{T_l} C_f dT+\int_{T_l}^{T_u}(C_i+L)dT+\int_{T_u}^{T} C_u dT & T_u< T\end{cases} \quad \text{(Eq. 3)}$$

The above enthalpy function is defined for a non-ideal material like biological tissue that changes phase over a range of temperature. Similar enthalpy functions can be defined for the ideal materials like water that changes phase at a constant temperature. On substituting Equation 5 in Equation 1, the governing equations for biological tissues for the frozen, unfrozen and mushy regions are obtained as follows

$$\textit{Unfrozen Region}\quad \frac{\partial H_u}{\partial t}=\bigtriangledown k_u\bigtriangledown T+S_m+S_b \qquad T\ge T_u \quad \text{(Eq. 4)}$$

$$\textit{Mushy Region}\quad \frac{\partial H_i}{\partial t}=\bigtriangledown k_i\bigtriangledown T \qquad T\le T_l \quad \text{(Eq. 5)}$$

$$\textit{Frozen Region}\quad \frac{\partial H_f}{\partial t}=\bigtriangledown k_f\bigtriangledown T \qquad T\le T_l \quad \text{(Eq. 6)}$$

For biological tissue freezing, the two biological heat sources of metabolism and blood perfusion are absent in the frozen and the mushy region. For water and bio-gel cryo-freezing, no heat source terms are present. The above equations are discretized based on control volume approach, and explicit time stepping scheme is used to numerically solve them. The time step is chosen small enough to satisfy the stability criteria of the explicit time stepping scheme and remove any oscillations present in the output.

Boundary and initial conditions

The initial temperature is assumed to be the body temperature of 37°C for biological tissue, and room temperature for water and bio-gel. The typical boundary conditions employed in the numerical simulations for biological tissue are illustrated in Figure 9 for a twodimensional cryo-freezing process.

The boundary condition at the cryogenic section of the probe is the most difficult to apply when simulating *in vivo* experiments. For the purpose of validation of the numerical code with laboratory experiments, the temperature readings at four locations of the cryoprobe are used as the boundary conditions. Linear interpolation is used to get the intermediate temperatures of the cryogenic section of the cryoprobe.

Numerical model validation

The developed numerical code is validated with three cases; 1) analytical solution for ideal material freezing, 2) laboratory experiments done using Probe2 in bio-gel as the phase change medium, and 3) experimental results of *in vivo* porcine liver cryosurgery done by Siefert et al. (2003).

Code validation with analytical solution. Exact analytical solutions for water freezing in one-dimensional semi-infinite domain was presented by Carslaw and Jaeger (1959). In brief, the problem consists of a semi-infinite 1D slab of water

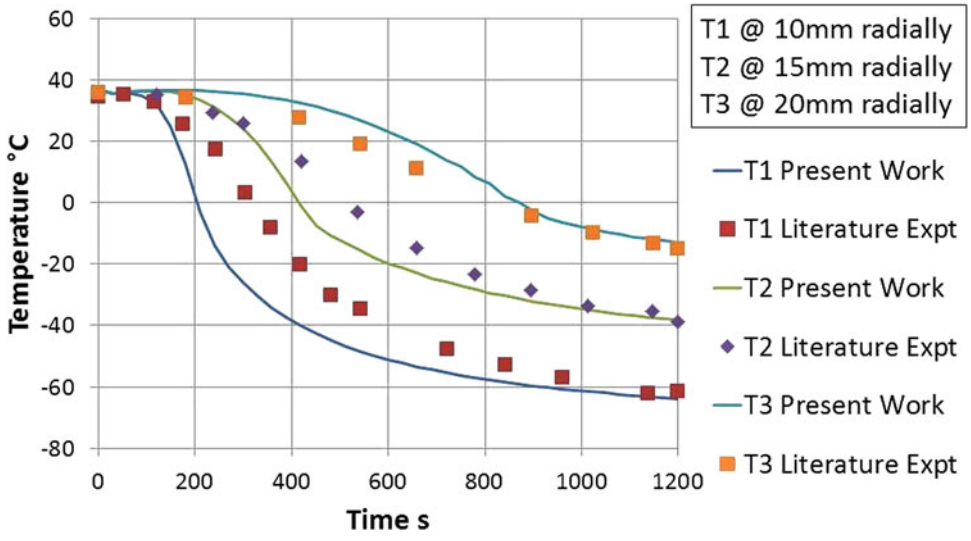

FIG. 12. Comparison of numerical code with cryo-freezing of porcine liver (Siefert et al., 2003).

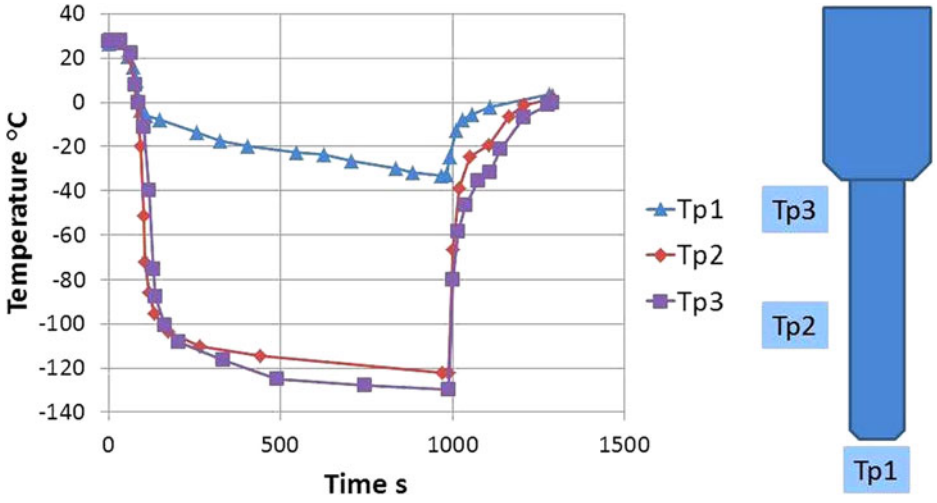

FIG. 13. Probe2 temperature profile with vapor separator.

initially at 10°C. At x = 0 the temperature is −20°C. In the numerical model the other end, at a distance of 4 m from x = 0, is assumed to be adiabatic. The two biological heat sources are absent in this case. Also the phase change occurs at a fixed temperature of 0°C as the working fluid is water. Figure 10 shows the comparison of the numerical results with the exact solution of Carslaw and Jaeger JC (1959). The numerical model matches well with the exact solution.

Code validation with laboratory experiments. The data of the bio-gel experiments obtained using the experimental set up with Probe2 attached to a vapor separator is compared with the predictions of the numerical code. The bio-gel is assumed to have water properties. The thermal conductivity and specific heat are taken to be temperature dependent. The comparison for temperatures sensors T1 and T2 is shown in Figure 11. It is to be seen that there is a good agreement between the numerical code prediction and experimental results.

Code validation with *in vivo* cryosurgery. The prediction of the developed code is also compared with *in vivo* experimental data from Seifert et al. (2003). Briefly, the experiment, as reported by Seifert et al., consists of 20 min freezing of porcine liver organ using an 8 mm-AccuProbeCryoprobe held at an approximately −175°C. The reader can refer to their work for further details regarding the experiments. Most of the biophysical properties used in the simulation are taken from published literature, while some that are not available in literature are assumed to be that of soft biological tissue. The properties are listed in Table 1. The temperature profiles from the simulation and experiment have been compared (Fig. 12). There is a reasonable match between the numerical code prediction and the experimental results.

The mismatch in numerical prediction with experimental results can be attributed to the following reasons

1. Assuming thermo-physical properties to be temperature independent;
2. Nonavailability of all the experimental data such as the temperature profile of the cryogenic section of the probe;
3. Experimental errors like heat conduction via thermocouples, etc.

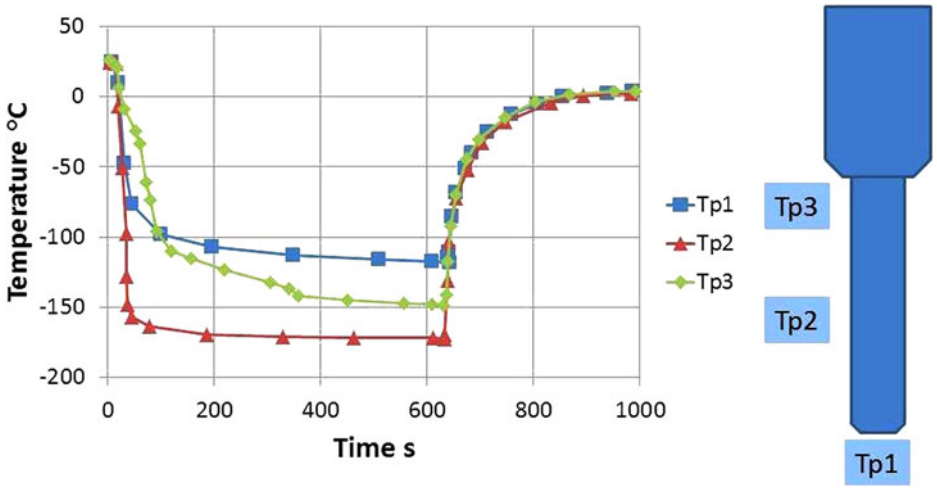

FIG. 14. Probe3 temperature profile without the vapor separator.

TABLE 2. EFFECT OF CRYOPROBE DIMENSIONS

	Water as the phase change medium		
	PROBE1	*PROBE2*	*PROBE3*
Minimum probe temperature	−60°C with vapor separator	−130°C with vapor separator	−170°C without vapor separator
Ice ball diameter after 15 min of freezing	23 mm	40 mm	50 mm for 10 min of freezing

Results and Discussion

The experimental results using the three cryoprobes, Probe1, Probe2, and Probe3, are presented. All the experiments comprised of 15 min of freezing followed by 5 min of thawing unless stated otherwise. The phase changing media used were water and bio-gel. Probe1 and Probe2 are attached to the vapor separator, whereas Probe3 is operated without a vapor separator. The numerical simulation results are also presented for further improvement.

Experimental results

Cryoprobe temperature profile. The experimental results for the temperature profile of the cryogenic section of the probes are shown in Figures 13 and 14. The experiments were conducted with water as the phase change medium. From above figures we can see that for low pressure LN2 cryoprobes the temperatures are not that close to the LN2 temperature. For Probe1 the minimum temperature using a vapor separator is −60°C. This can be attributed to the reduced mass flow rate in low pressure cryoprobes.

From Figures 13 and 14 one can also see that temperature Tp1 at the tip of the cryoprobe is considerably warmer than the rest of the cryogenic section of the probe. This effect is said to occur due to the formation of a thin gas layer at the tip where change in direction of the flow occurs.

Effect of cryoprobe dimensions. The experimental results using the three cryoprobes are summarized in Table 2. Probe1 and Probe2 have the same cryogenic section diameter, but Probe2 is larger in the vacuum insulated section. Probe3 is larger than Probe1 and Probe in the cryogenic and the vacuum insulated section. From the table, it can be seen that, with increase in probe diameter, there is a decrease in the minimum probe temperature and the iceball diameter is also larger. Thus a larger diameter low pressure LN2 cryoprobe is able to produce more cryogenic injury within the same time but at the cost of increased invasiveness whereas the smaller diameter low pressure LN2 cryoprobes are not able to achieve the same.

Effect of vapor separator. Vapor separator is used to remove the vapor lock and decrease the precooling time. The vapor lock effect is more prominent in smaller diameter probes; therefore vapor separator is more effective in smaller diameter probes. Figure 15 shows the cryogenic section temperature profile at 4 mm from the tip of Probe1 with and without the Vapor Separator.

From Figure 15, we can see that without the vapor separator there is hardly any drop in the probe temperature; whereas with the vapor separator the probe temperature drops instantaneously to about −40°C and the minimum temperature attained is −60°C. For Probe2 the minimum temperature with and without vapor separator are −130°C and −80°C, respectively. Probe3 can reach −170°C without a vapor separator. Thus the vapor separator is seen to be effective for smaller diameter cryoprobes.

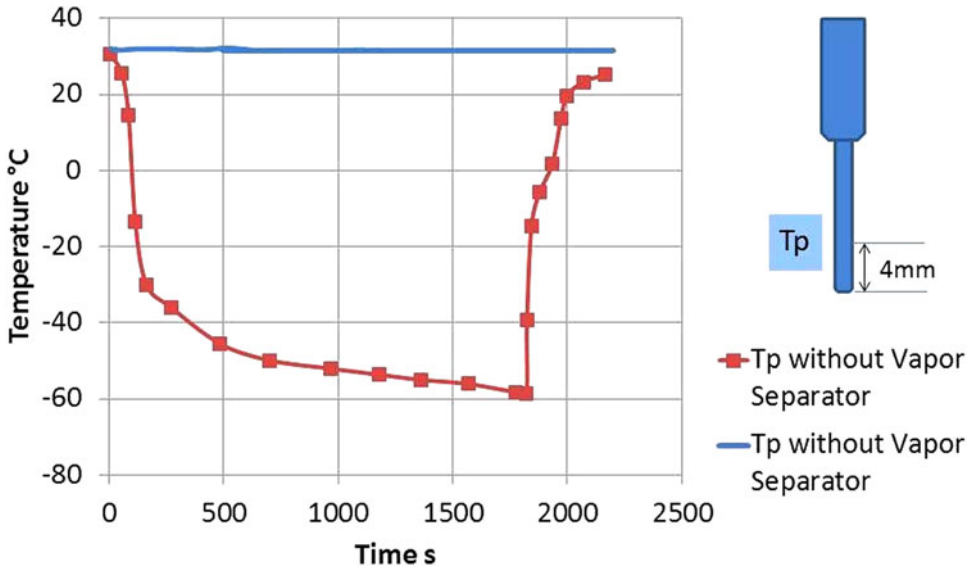

FIG. 15. Effect of vapor separator on Probe1.

Table 3. Effect of Phase Change Medium

	Probe2 with vapor separator	
Phase changing medium	*Water*	*Bio-gel*
Minimum probe temperature	−130°C	−150°C
Ice ball diameter after 15 min of freezing	40 mm	53 mm

Effect of phase change medium/cooling load. Table 3 shows the minimum probe temperature and the maximum iceball diameter at the end of 15 min freezing for Probe2 with a vapor separator. The experiments are performed to evaluate the probe performance under different heating loads. Water and bio-gel are used as the two phase changing mediums representing higher and lower cooling loads. The convective currents in water are an additional heat load as compared to bio-gel medium in which there is pure conduction. From Table 3 we can see that higher cooling loads result in warmer cryoprobe temperatures and consequently smaller iceball diameters.

Numerical simulation

Experiments have shown that Probe2 attains a minimum temperature of −130°C in water and −150°C in bio-gel. The developed numerical code is used to investigate the effect of reaching lower probe temperatures with the same dimensions of Probe2.

Figure 16 shows the numerical problem statement. It consists of a cancerous tumor of 22 mm diameter placed centrally around Probe2. The biophysical properties are taken of porcine liver. The edge of the tumor in the radial direction along the center of the cryogenic section is represented by point A. To investigate the effect of lower probe temperatures, the steady state temperature of Probe2 in water is reduced to −196°C (saturated LN2 temperature) in the numerical model. Figure 17 shows the numerical prediction of the growth of −50°C isotherm (critical isotherm) and Tu isotherm (upper phase change temperature isotherm) for the cooler (-196°C) and warmer (-130°C) cryoprobes. The gap between the Tu isotherm and −50°C isotherm represents the buffer zone.

The critical isotherm of the cooler probe reaches the tumor edge (point A) in about 360s, whereas the warmer probe takes 750s.

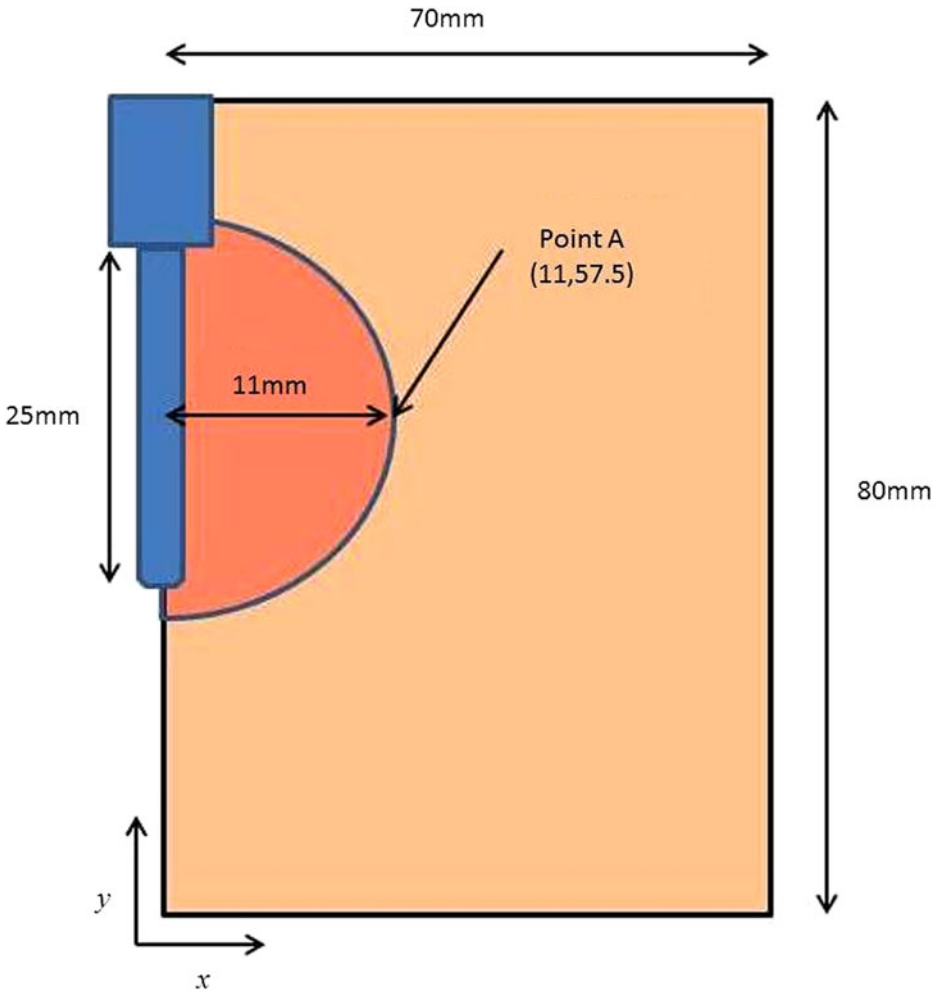

FIG. 16. Numerical domain to investigate the effect of reaching lower probe temperatures.

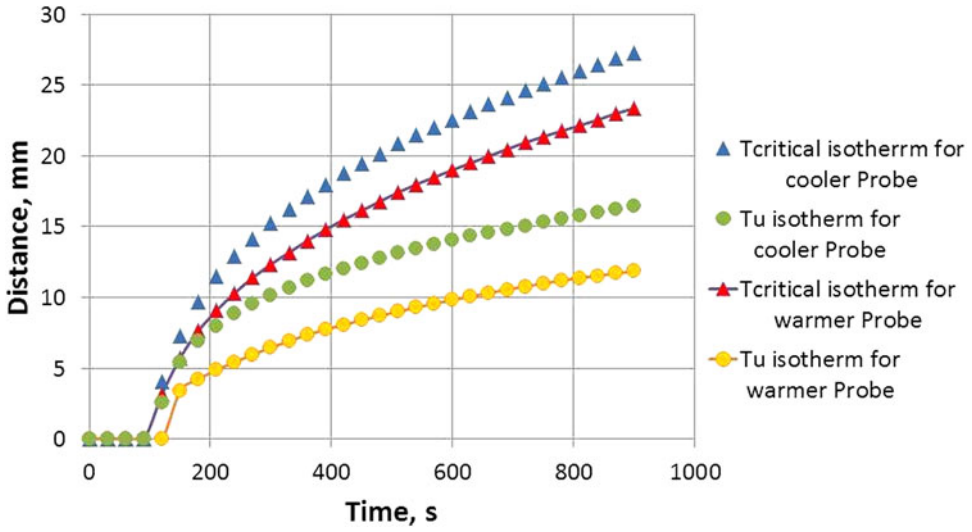

FIG. 17. Growth of the critical and Tu isotherm for cooler and warmer cryoprobes.

The size of the buffer zone when the critical isotherm reaches the tumor is i) 10.4 mm for the warmer probe and ii) 6 mm for the cooler probe. Thus there is a 42% reduction in the size of buffer zone. In effect we can say that the buffer zone size is smaller for the cooler probe and the time taken to completely destroy the 22 mm diameter tumor is also less in the case of the cooler probe. Thus a cooler probe of the same dimensions (invasiveness) and producing lower temperatures results in a larger iceball in shorter time while minimizing the volume of the buffer zone within the iceball, which is more efficient in a cryosurgical process.

We report here for the first time both in-silico and empirical parameters of iceball formation around a cryosurgical medical device. Because the iceball formed is directly pertinent for, and a precursor event to cancer cell destruction, these findings may lead to the ways in which future cryosurgical devices can be designed.

Conclusions

To the best of our knowledge, this is the first report that describes the formation of iceball for a future cryosurgical medical device of significant relevance for cancer therapeutics. Specifically, we developed three low pressure LN2 cryoprobes. The smaller diameter probes (3 mm) produce warmer temperatures as compared to larger diameter LN2 cryoprobes. Consequently the iceball growth is larger and faster in larger diameter cryoprobes. Low pressure and smaller diameter LN2 cryoprobes face the problem of vapor lock. Vapor separator is found to be very effective in removing the same and reducing the precooling time. Larger diameter cryoprobes (11 mm) do not show any vapor lock and hence there is no need of vapor separator. Low pressure LN2 cryoprobes show lower probe temperatures for low cooling loads and consequently produce larger and faster iceball diameters.

An enthalpy-based numerical code for phase change heat transfer is developed to simulate the cryosurgical process. The numerical code is compared with 1D analytical solution; laboratory experiments using Probe2 along with the vapor separator in bio-gel; and also with experimental results of *in vivo* liver cryosurgery. The numerical code shows very good agreement with analytical solution results. There is also a reasonable match of the numerical predictions with the laboratory experiments and *in vivo* liver cryosurgery. Numerical investigation using the developed code shows that production of lower probe temperatures results in a more efficient cryosurgical process. LN2 cryoprobes producing cooler temperatures result in a reduction in the size of the buffer zone and also in the time of surgery.

Author Disclosure Statement

The authors declare that there are no conflicting financial interests.

References

Carslaw HS, and Jaeger JC. (1959). *Conduction of Heat in Solids,* 2nd ed. Clarendon Press, London, pp. 282–295.

Choi J, and Bischof JC. (2010). Review of biomaterial thermal property measurements in the cryogenic regime and their use for prediction of equilibrium and non-equilibrium freezing applications in cryobiology. Cryobiology 60, 52–70.

Gage AA, and Baust J. (1988). Mechanisms of tissue injury in cryosurgery. Cryobiology 37, 171–186.

Kumar S, and Katiyar VK. (2007). Numerical study on phase change heat transfer during combined hyperthermia and cryosurgical treatment of lung cancer. Intl J Appl Math Mech 3, 1–17.

Lee CY, and Bastacky J. (1995). Comparative mathematical analyses of freezing in lung and solid tissue. Cryobiology 32, 299–305.

Mazur P. (1984). Freezing of living cells: Mechanisms and implications. Am J Physiol 247 (Cell Physiol 16), C125–C142.

Pennes HH. (1948). Analysis of tissue and arterial blood temperatures in the resting forearm. J Appl Physiol 1, 93–100.

Rubinsky B. (2000). Cryosurgery. Ann Rev Biomed Engineer 2, 157–187.

Seifert JK, Gerharz CD, Mattes F, et al. (2003). A pig model of hepatic cryotherapy: In vivo temperature distribution during

freezing and histopathological changes. Cryobiology 47, 214–226.

Zhao G, Luo DW, Liu ZF, and Gao DY. (2007). Comparative study of the cryosurgical processes with two different cryosurgical systems: The Endocare Cryoprobe System versus the Novel Combined Cryosurgery and Hyperthermia System. Latin Am Appl Res 37, 215–222.

Address correspondence to:
Professor Milind D. Atrey
Department of Mechanical Engineering
IIT Bombay
Powai
Mumbai 400 076
India

E-mail: matrey@iitb.ac.in